P-loop Flexibility in Na^+ Channel Pores Revealed by Single- and Double-cysteine Replacements

Robert G. Tsushima, Ronald A. Li, and Peter H. Backx

From the Department of Medicine and The Centre for Cardiovascular Research, University of Toronto, Toronto, Ontario M5G 2C4, Canada

ABSTRACT Replacement of individual P-loop residues with cysteines in rat skeletal muscle Na^+ channels (SkM1) caused an increased sensitivity to current blockade by Cd^{2+} thus allowing detection of residues lining the pore. Simultaneous replacement of two residues in distinct P-loops created channels with enhanced and reduced sensitivity to Cd^{2+} block relative to the individual single mutants, suggesting coordinated Cd^{2+} binding and cross-linking by the inserted sulfhydryl pairs. Double-mutant channels with reduced sensitivity to Cd^{2+} block showed enhanced sensitivity after the application of sulfhydryl reducing agents. These results allow identification of residue pairs capable of approaching one another to within less than 3.5 Å. We often observed that multiple consecutive adjacent residues in one P-loop could coordinately bind Cd^{2+} with a single residue in another P-loop. These results suggest that, on the time-scale of Cd^{2+} binding to mutant Na^+ channels, P-loops show a high degree of flexibility.

KEY WORDS: Na^+ channels • structure • Cd^{2+} binding • mutagenesis • *Xenopus* oocytes

INTRODUCTION

Previous modelling (Noda et al., 1984; Hille, 1992; Lipkind and Fozzard, 1994; Guy and Durell, 1995; Soman et al., 1995) and mutagenesis experiments (Terlau et al., 1991; Backx et al., 1992; Heinemann et al., 1992; Satin et al., 1992) have established that P-loops are critical determinants of catalytic permeation properties of Na^+ channels, but their precise molecular structure is unknown (Guy and Durell, 1994). These P-loops are located between S5 and S6 in the four homologous repeat domains of Na^+ (Noda et al., 1984) and Ca^{2+} channels (Ellinor et al., 1995) and are located at analogous positions in K^+ (MacKinnon and Miller, 1989) and cyclic nucleotide-gated channels (Heginbotham et al., 1992; Sun et al., 1996). Four P-loops, pseudo-symmetrically arranged, are necessary to form a functional pore (MacKinnon, 1991; Catterall, 1995). While other regions, such as the fifth (S5) and sixth transmembrane (S6) segments (Lopez et al., 1994) as well as the S4-S5 loops (Isacoff et al., 1991) of voltage-gated channels influence permeation, P-loops are critical determinants of ion selectivity. Based on mutagenesis experiments, various structural models for P-loop backbones have been proposed: β-strands with β-hairpin loops (Yellen et al., 1991; Lipkind and Fozzard, 1994; Soman et al., 1995), random coils (Sun et al., 1995; Perez-Garcia et al., 1996) and α-helices with β-turns (Guy and Durell, 1995). More recently, detailed three-dimensional information on the relationship of P-loop residues to one another has been obtained using mutant cycling analysis of toxin binding to channels (MacKinnon and Miller, 1989; Gross and MacKinnon, 1995; Hidalgo and MacKinnon, 1995; Ranganathan et al., 1996).

In this manuscript we assess the molecular architecture of the pore by using Cd^{2+} as a biophysical probe of mutant channels in which one or two P-loops residues are replaced by cysteines. Cd^{2+} was chosen because: (*a*) its ionic radius (0.92 Å) (Cotton and Wilkinson, 1992) is nearly identical to Na^+ (0.95 Å), (*b*) it binds free sulfhydryls with high affinity in a "near-covalent" manner (Cotton and Wilkinson, 1992), and (*c*) it can coordinately bind to multiple free sulfhydryls with a tetrahedral geometry, as observed in Zn^{2+}-finger proteins (Vallee and Falchuk, 1993) and metallothioneins (Shaw et al., 1992), while binding very weakly to oxidized sulfhydryls (Torchinsky, 1981). Thus, Cd^{2+} is well suited for identifying P-loop residues lining the Na^+ channel pore after cysteine replacement. Furthermore, Cd^{2+} can be used to evaluate the spatial relationship between pairs of residues in channel pores by simultaneously replacing two P-loop residues by cysteine. In these double-cysteine mutant channels, changes in sensitivity to Cd^{2+} block of ionic currents, compared to single-cysteine mutants, can identify residue pairs capable of interacting by coordinately binding Cd^{2+} or forming disulfide linkages. A similar strategy was also recently used by Benitah et al. (1996) in Na^+ channels and Krovetz et al. (1997) in K^+ channels to determine residue proximity.

In our studies, the pattern of P-loop residue pairs able to coordinately bind Cd^{2+} or form disulfide bonds demonstrates that P-loops are remarkably flexible on

Address correspondence to Dr. Peter H. Backx, Department of Medicine, Cardiovascular Research, Toronto General Hospital, 101 College Street, CCRW 3-802, Toronto, Ontario M5G 1L7, Canada. Fax: 416-340-4596; E-mail: pbackx@utoronto.ca

Robert G. Tsushima and Ronald A. Li contributed equally to this manuscript.

the time-scale of Cd^{2+} binding and coordination. Our observations are not unexpected, especially given the analogy between ion channels and enzymes (Eisenberg, 1990; Miller, 1992); ion channel pores are the active sites which catalyze the selective passage of ions across the cell membrane (Eisenberg, 1990; Miller, 1992). Indeed, many well studied enzymes have active sites formed by highly flexible "random-coil" loop structures (Branden and Tooze, 1991; Creighton, 1993), and flexibility is crucial for both selective substrate binding and catalytic activity (Pompliano et al., 1990; Lan et al., 1995; Larson et al., 1995; Nicholson et al., 1995).

METHODS

Molecular Biology

For mutagenesis fragments of the SkM1 rat skeletal muscle Na^+ channel (Trimmer et al., 1989) were subcloned into pGEM-11f or pGEM-7f (Promega Corp., Madison, WI). Uracil-enriched single-stranded templates were used to introduce site-specific cysteine substitutions (Kunkel, 1985). The mutated fragments were sequenced (Sequenase; United States Biochemical Corp., Cleveland, OH) before subcloning into the expression vector GW1H (British Biolabs, Oxford, UK) containing the full length Na^+ channel clone. Mutants were also re-sequenced in the expression vector to ensure the desired point mutation was present. Nuclei of stage V-VI oocytes obtained from *Xenopus laevis* were injected with 0.1–0.5 ng of column purified (Qiagen Inc., Chatsworth, CA) plasmid DNA. Double-cysteine mutants were created by ligating single-cysteine mutants located in D-I with single-cysteine mutants in D-II, D-III, and D-IV. The double-cysteine mutants were re-sequenced in the P-loop regions to confirm that the desired mutations were present.

Electrophysiology

Whole-cell currents from oocytes were measured in response to depolarizations from a holding potential of −120 mV using two-electrode voltage-clamp recordings (Warner Instruments, Hamden, CT). Electrode pipettes were fabricated from 1.2-mm outer diameter thin-walled borosilicate glass (TW120F-6; World Precision Instruments, Inc., Sarasota, FL) pulled on a Sutter puller (model P-87; Sutter Instruments, Co., Novato, CA). Pipette tips were plugged with 1% agarose (in 3 M KCl) and had a final resistance of 0.5–2 MΩ. Leak subtraction was accomplished using a P/8 protocol from a holding potential of −120 mV. Currents were filtered at 2 kHz and digitized at 10 kHz. To minimize difficulties associated with adequately voltage-clamping oocytes which expressed large numbers of channels, whole-cell recordings were limited to oocytes expressing less than 5 μA of peak current. The oocytes were bathed in a solution (ND96) containing: 96 mM NaCl, 5 mM HEPES (pH = 7.6, NaOH), 1 mM $MgCl_2$, 1 mM $BaCl_2$. Variable concentrations of $CdCl_2$ were added as required. We also added, when needed, methane-thiosulfate-ethylammonium (MTSEA) at a concentration of 1 mM and dithiothreitol at a concentration of 10 mM. The application of MTSEA and DTT was achieved by washing at least 30 ml of solution while the oocytes were depolarized every 2 s to −10 mV from a holding potential of −120 mV. All whole-cell experiments were done at pH = 7.6 and at 21–23°C.

Single-channel recordings were idealized by using the 50% amplitude criterion to identify channel openings and closings. Idealized channel openings were used to construct unblocked- and blocked-time density distribution histograms and the number of openings per sweep (Colquhoun and Sigworth, 1983). Mean unblocked-times were estimated by fitting unblocked-time density histograms to a mono-exponential function using a nonlinear least-squared algorithm. Mean blocked-times were estimated by fitting the blocked-time histogram with either a mono-exponential or a bi-exponential function (Colquhoun and Sigworth, 1983). The goodness of fit was estimated by calculating the F-statistic and using the F-distribution ($p < 0.05$). For all the single-channel patches studied, the unblocked-time histograms were suitable while bi-exponential fits were required for double-cysteine mutants.

Curve Fitting and Statistics

The dissociation constant, K_D, for Cd^{2+} binding to the channel was estimated using least-squares fitting of the dose-response curves to the equation: $G/G_o = K_D/(K_D + [Cd^{2+}])$, where G and G_o represent measured Na^+ conductance in the presence and absence of Cd^{2+}, respectively. The conductance was estimated from the slope of the linear portion of the current-voltage relationship as previously described (Tsushima et al., 1997). Statistical significance for the changes in Cd^{2+} binding was determined by comparing the experimentally estimated K_D (mean ± SD) between single-cysteine mutant and wild-type Skm1 (i.e., WT) channels using a paired Student's t test ($p < 0.05$).

When Cd^{2+} binds independently to the two cysteines inserted into P-loops of distinct domains of the Na^+ channels we expect the dissociation constant for Cd^+ block of Na^+ current to be directly determined by the dissociation constants measured for the individual single-cysteine mutants. Specifically, the predicted dissociation constants for the double-mutant, $K_{D,pre}$, for independent binding of Cd^{2+} to the two cysteines is given by the equation:

$$1/K_{D,pre} = 1/K_D{}^1 + 1/K_D{}^2, \quad (1)$$

where $K_D{}^1$ and $K_D{}^2$ represent the estimated dissociation constants for the single-cysteine mutants 1 and 2. Therefore, $K_{D,pre}$ was compared to the measured dissociation constant (i.e., $K_{D,ob}$) in order to assess whether coordinated Cd^{2+} binding occurred in the double-cysteine mutants. A one-way analysis of variance for three groups was employed (Bogartz, 1994) in order to assess whether the measured mean of $1/K_{D,ob}$ differed statistically from the estimated mean $1/K_{D,pre}$ predicted from Eq. 1. This test took into account the measured variance of $K_D{}^1$, $K_D{}^2$, and $K_{D,ob}$ in determining statistical significance ($p < 0.05$).

When the two inserted cysteine residues are capable of simultaneously binding a Cd^{2+} ion, the observed dissociation constant for Cd^{2+} binding will be reduced compared to $K_{D,pre}$. Indeed, under such circumstances the dissociation constant for the double-mutant channel, $K_{D,co}$, is given by:

$$K_{D,co} = K_D{}^1 \cdot \exp[-(\delta G_2 + \delta G_d)/kT] = K_D{}^2 \cdot \exp[-(\delta G_1 + \delta G_d)/kT], \quad (2)$$

where δG_1 and δG_2 are the free energies of Cd^{2+} binding to sites 1 and 2, respectively (expected to be negative), δG_d is the distortional and entropic free energies required for the protein to coordinately bind Cd^{2+} (expected to be positive), k is Boltzmann's constant, and T is the absolute temperature. Thus for coordinated Cd^{2+} binding, $(\delta G_2 + \delta G_d)$ and $(\delta G_1 + \delta G_d)$ represent the stabilization energy contributed by Cd^{2+} binding to the second site. Therefore, the average stabilization energy for coordinated Cd^{2+} binding could be directly obtained from measurements of $K_D{}^1$, $K_D{}^2$, and $K_{D,ob}$.

RESULTS

Single-cysteine Substitutions of P-loops Residues

Single-cysteine mutant channels were created (Akabas et al., 1992) and probed with both Cd^{2+} and sulfhydryl-reactive compounds in order to identify side-chains of P-loop residues which line the pore. All single-cysteine replacements studied (Fig. 1), except G1238C, produced functional channels with normal gating properties. Fig. 2 *A* shows scaled sample Na^+ currents measured in oocytes before (*solid line*) and after (*broken line*) extracellular addition of 100 μM extracellular Cd^{2+} in wild type (WT), Y401C, W402C, and E403C. Clearly, all three mutants have an elevated sensitivity to Cd^{2+} compared to the wild type. This is more clearly illustrated in Fig. 2 *B* which displays the relative whole-cell conductance at varied extracellular [Cd^{2+}] for the wild type and three mutants shown in Fig. 2 *A*. From such dose response, estimates of the dissociation constant for Cd^{2+} binding to the channel pore are obtained as outlined in the methods. To quantify the increase in sensitivity to Cd^{2+} of mutant channels, where P-loop residues are replaced by cysteine, Fig. 2 *C* shows the ratio of the estimated mean dissociation constant for the single-cysteine mutants ($K_{D,Mut}$) to the wild-type ($K_{D,WT}$) measured before (*filled bars*) and after (*open bars*) oxidation with external application of MTSEA. Table I lists the measured dissociations constants (i.e., mean ± SD) for the same channels. All channels (except W756C) had significantly ($p < 0.01$) increased sensitivity to block by Cd^{2+} (i.e., smaller dissociation constants, K_D) compared to WT channels (Fig. 2 *B*). Extracellular application of 1 mM MTSEA for a period of 5–7 min, which rapidly modifies free sulfhydryls by forming disulfide complexes (Akabas et al., 1992), abolished high affinity block by Cd^{2+} (Fig. 2 *C*). This establishes that enhanced Cd^{2+}-sensitivity depends on the free sulfhydryls inserted into the pore since Cd^{2+} binds weakly to oxidized sulfhydryls (Torchinsky, 1981). The elimination of Cd^{2+} sensitivity by MTSEA could be readily reversed by the application of the sulfhydryl reducing agent dithiothreitol (DTT) at a concentration of 10 mM while reduction with DTT did not affect channels not previously exposed to MTSEA (data not shown). Clearly, two, three, or four adjacent consecutive P-loop residues have their side-chains exposed to the external face of

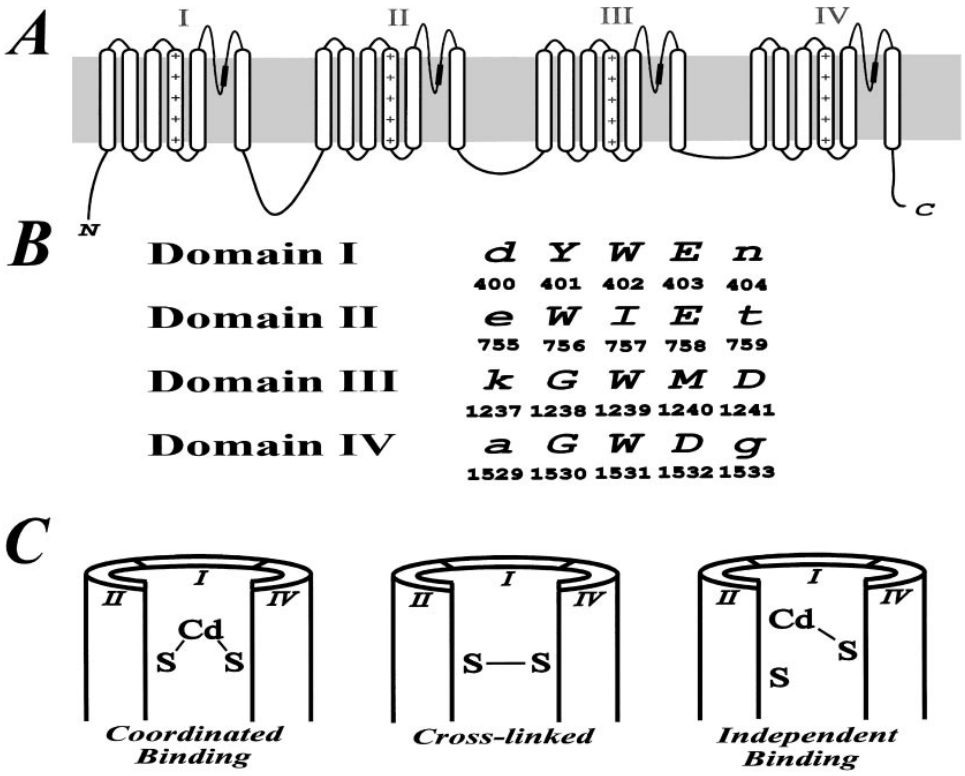

FIGURE 1. (*A*) The putative topology of Na^+ channels showing four homologous internal repeats each with six transmembrane segments (S1-S6). The four P-loops which are located between S5 and S6 in each repeat domain form a major part of the channel pore. The approximate location of residues mutated in our study are marked by a thickened portion of the COOH-terminal portion of the P-loop (i.e., SS2 domain). (*B*) Partial alignment sequences along with the corresponding residue numbers of the P-loops in the region which were mutated in our experiments. The mutated residues are marked as capital letters. (*C*) Three outcomes of introducing pairs of cysteine residues into distinct homologous repeat domains of Na^+ channels are possible. Coordinated Cd^{2+} binding is expected if the two inserted sulfhydryls are sufficiently close to one another. Cross-linked channels are expected to be insensitive to current block by Cd^{2+} and will become more Cd^{2+}-sensitive by reduction with DTT. If the two inserted cysteines are distant from one another, we expect Cd^{2+} to bind independently.

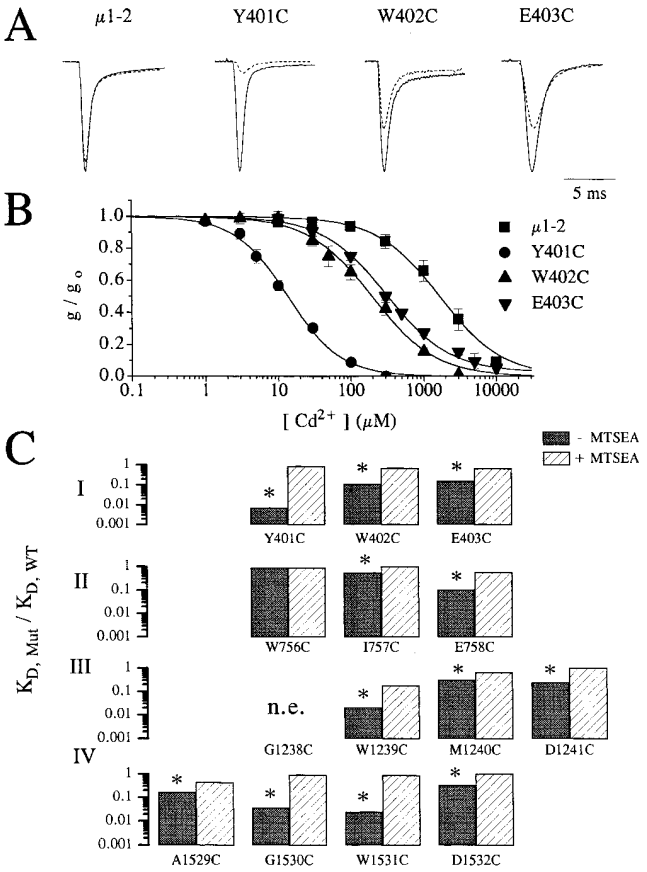

FIGURE 2. (*A*) Raw current traces of wild-type, Y401C, W402C, and E403C channels recorded in oocytes following depolarization to −10 mV from a holding potential of −120 mV with (*broken line*) and without (*solid line*) 100 μM extracellular Cd^{2+}. Clearly, the amount of current reduction is much greater for the mutant channels (*Y401C*, *W402C*, and *E403C*) than for the wild-type channels. The currents amplitudes have been scaled for ease of comparison. Peak currents in μA were: 3.8 (*WT*), 3.5 (*Y401C*), 3.5 (*W402C*), and 2.0 (*E403C*). (*B*) Plots of the fraction of peak current remaining as a function of the extracellular [Cd^{2+}] for the same channels shown in *A*. Curve fits allow estimation of the dissociation constants (i.e., K_D) for Cd^{2+} binding to the channel pore. (*C*) Summary of the Cd^{2+} block in single-cysteine mutants. The ratio of the estimated K_D for Cd^{2+} block of current in single-cysteine mutants divided by the wild-type channels (i.e., $K_{D,mut}/K_{D,WT}$) for control conditions (*filled bars*) and following the application of 1.0 mM methane-thiosulfate-ethylammonium (*MTSEA*) to oxidize the inserted free sulfhydryls (*open bars*). For each mutant, except W756C, $K_{D,mut}$ was significantly reduced ($p < 0.001$) more than 3-fold, which was abolished by the application of MTSEA.

TABLE I

Dissociation Constants (K_D) for Cd^{2+} of WT and Mutant Na^+ Channels before and after MTSEA Modification

Mutants	IC_{50} (μM)	IC_{50} (μM) after MTSEA modification
WT (SkM1)	$1.8 \pm 0.4 \times 10^3$ (3)	N/A
Y401C	1.3 ± 0.3 (5)	$1.6 \pm 0.1 \times 10^3$ (3)
W402C	$2.0 \pm 0.1 \times 10^2$ (4)	$1.2 \pm 0.1 \times 10^3$ (3)
E403C	$2.8 \pm 0.2 \times 10^2$ (5)	$1.2 \pm 0.2 \times 10^3$ (5)
W756C	$1.6 \pm 0.1 \times 10^3$ (4)	$1.6 \pm 0.4 \times 10^3$ (2)
I757C	$2.0 \pm 0.2 \times 10^2$ (2)	$8.8 \pm 0.7 \times 10^2$ (3)
E758C	$4.9 \pm 0.3 \times 10^2$ (8)	$1.0 \pm 0.1 \times 10^3$ (3)
G1238C	n.e.	n.e.
W1239C	$3.7 \pm 1.0 \times 10$ (3)	$3.2 \pm 0.3 \times 10^2$ (2)
M1240C	5.7 ± 0.3 (5)	$1.2 \pm 0.1 \times 10^3$ (2)
D1241C	$4.5 \pm 0.5 \times 10^2$ (3)	$1.9 \pm 0.3 \times 10^3$ (3)
A1529C	$3.0 \pm 0.6 \times 10^2$ (3)	$8.0 \pm 0.6 \times 10^2$ (2)
G1530C	$6.8 \pm 0.9 \times 10$ (4)	$1.7 \pm 0.2 \times 10^3$ (3)
W1531C	$4.6 \pm 0.5 \times 10$ (5)	$1.6 \pm 0.3 \times 10^3$ (6)
D1532C	$6.0 \pm 0.7 \times 10^2$ (8)	$2.3 \pm 0.3 \times 10^3$ (2)

Numbers in parentheses represent number of determinations. n.e., no expression.

the permeation pathway thereby allowing interactions with extracellularly applied Cd^{2+} ions. At first glance these results, which are similar to results in other ion channels (Akabas et al., 1992; Gross and MacKinnon, 1995; Kurz et al., 1995; Pascual et al., 1995; Perez-Garcia et al., 1996), are difficult to reconcile with α-helical or β-strand 2° structures, but only provided P-loops are relatively rigid and immobile. However, as shown below, the assumption of P-loop immobility is not valid on the time-scale of sulfhydryl modification and Cd^{2+} binding.

A comparison of the $K_{D,Mut}/K_{D,WT}$ ratio between different mutants in Fig. 2 *C* uncovers unexpected differences between residues in homologously aligned locations from distinct P-loops (Fig. 1). For example, Y401C is exquisitely sensitive to Cd^{2+} in comparison to W756C, which has wild-type sensitivity whereas G1530C has intermediate sensitivity. Furthermore, mutant channels with cysteine replacements at homologous alignment locations in different repeat domains do not generally have similar affinities for Cd^{2+} binding. These results argue against a symmetrical arrangement of the residues at equivalent alignment locations between P-loops of different domains. In spite of large variations in Cd^{2+}-sensitivity between different single-cysteine mutants, MTSEA was able to access all mutated residues as measured by the elimination of high affinity Cd^{2+} block, providing additional support for the conclusion that these P-loop residues are exposed to the extracellular face of the pore.

Double-cysteine Substitution of P-loops Residues from Distinct Internal Repeat Domains

To discriminate further between various models for the P-loop structure and to obtain detailed three-dimensional relationships between various pore-lining residues, double-cysteine mutants were created by combining single-cysteine mutants from distinct P-loops. Since coordinated Cd^{2+} binding and disulfide cross-linking of the two nearby inserted cysteines require very restricted geometries (i.e., S-Cd^{2+} bonds are 2.1 Å and

S-Cd^{2+}-S angles are 108° while S-S bonds are 2.05 Å and the angle between two C_β-S bonds is 70–100°) (Torchinsky, 1981; Balaji et al., 1989; Careaga and Falke, 1992), these double-mutant channels provide an opportunity to determine detailed structural information on spatial relationship between side-chains of pore residues (Benitah et al., 1996; Krovetz et al., 1997).

Fig. 1 *C* illustrates the three potential outcomes expected following insertion of cysteine pairs into the channel pore. First, if the two inserted sulfhydryls are correctly spatially oriented, coordinated Cd^{2+} binding will occur and thereby enhance sensitivity to Cd^{2+} block of current compared to single-cysteine mutants (Cotton and Wilkinson, 1992; Vallee and Falchuk, 1993). Enhanced Cd^{2+} binding results from the stabilization energy derived from the formation of two simultaneous bonds between the Cd^{2+} ion and the two free sulfhydryls as described by Eq. 2 (METHODS). Alternatively, cross-linking of proximal inserted cysteines, which is strongly favored by the oxidizing extracellular environment (Fig. 2), will create relatively Cd^{2+}-insensitive cross-linked channels and these channels will become Cd^{+}-sensitive after DTT application. Finally, if the substituted cysteines are sufficiently far apart, Cd^{2+} will bind independently and, in that case, the dissociation constant for Cd^{2+} block of whole-cell current can be predicted (i.e., $K_{D,pre}$) from the sensitivity of the single-cysteine mutants as described by Eq. 1 (METHODS). Therefore, when the ratio of the experimentally observed K_D (i.e., $K_{D,ob}$) to $K_{D,pre}$ is significantly different from 1, evidence for either cross-linking or coordinated Cd^{2+} binding is obtained.

Remarkably, all double-cysteine mutant channels created (except W402C/I757C and those constructed with G1238C) formed functional channels. Fig. 3, *A* and *B*, presents typical results for Y401C/E758C channels; the measured dissociation constant for Cd^{2+} block ($K_{D,ob}$) for Y401C/E758C channels was 1,353 ± 382 μM (mean ± SD, $n = 7$) compared to 12 μM predicted for independent binding (i.e., K_D(Y401C) = 13.7 ± 3.0 μM ($n = 6$) and K_D(E758C) = 454 ± 47 μM ($n = 7$)). Following reduction with 10 mM DTT, applied for a period of 8–10 min, the K_D for Cd^{2+} block decrease about 1,200-fold to 1.1 ± 0.2 μM ($n = 4$). In this mutant, DTT increased the whole-cell current about 2.5-fold; DTT washin also caused comparatively large increases in whole-cell current and/or conductance in other cross-linked mutant channels studied. The increase in current invariably occurred in less than 30 s after DTT application, indicating rapid separation of the cross-linked cysteines. Furthermore, reduction with DTT enhanced the sensitivity of cross-linked channels to Cd^{2+} blockade (see below). Subsequent to DTT-reduction, Cd^{2+}-sensitive Y401C/E758C and other cross-linked double-cysteine channels could be made Cd^{2+}-insensitive again by applying 1 mM MTSEA (data not shown).

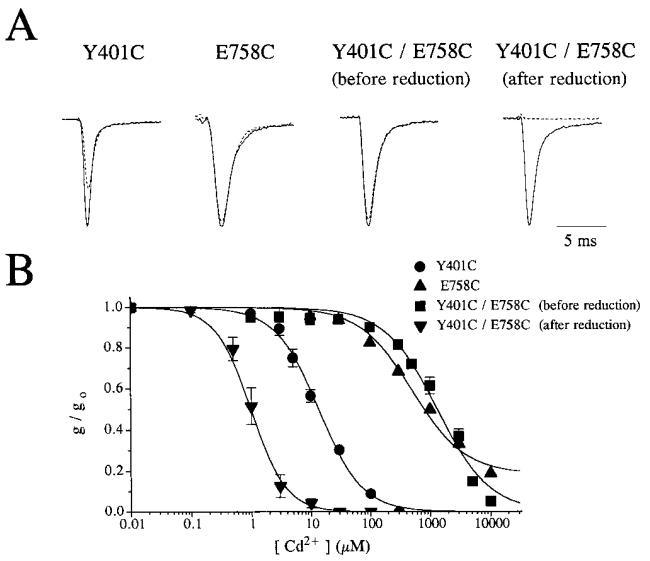

FIGURE 3. (*A*) Na^+ current tracings of Y401C, E758C, and Y401C/E758C mutant channels in response to depolarization to −10 mV from a holding potential of −120 mV before (*solid traces*) and after (*broken traces*) the addition of 100 μM Cd^{2+}. Na^+ currents for Y401C/E758C channels are shown before and after the addition of DTT. The currents have been scaled for ease of comparison. The current amplitudes in the absence of Cd^{2+} were (μA): 3.5 (Y401C), 2.7 (E758C), 2.2 (Y401C/E758C −DTT), and 4.6 (Y401C/E758C + DTT). (*B*) Dose-response curves of the normalized peak Na^+ current as a function of the [Cd^{2+}]. The channels become about 1,200-fold more sensitive to Cd^{2+} (K_D changes from 1,353 ± 382 μM to 1.1 ± 0.2 μM) following the addition of 2 mM DTT.

Data for the double-cysteine mutants created with Y401C, W402C, and E403C are summarized in Fig. 4, which depicts the ratio of the experimentally measured $K_{D,ob}$ for Cd^{2+} binding to double-cysteine mutant channels divided by the predicted $K_{D,pre}$ before (*filled bars*) and after (*open bars*) the application of DTT. Table II lists the measured $K_{D,ob}$ values (i.e., mean ± SD). Many double-mutants showed evidence for disulfide cross-linking: $K_{D,ob}/K_{D,pre}$ was above 1 before DTT and/or decreased significantly after DTT application in E403C/E758C, A1529C, G1530C, W1531C, D1532C, and Y401C/E758C, A1529C channels. We conclude that the inserted sulfhydryls in these double mutants are able to approach one another to within 2.05 Å under oxidizing conditions. Following the application of 10 mM DTT for 8–10 min, cross-linked double-mutants became ultra-sensitive to Cd^{2+} application compared to the corresponding single-mutants indicating an ability to coordinately bind Cd^{2+}. Double-mutants having $K_{D,ob}/K_{D,pre}$ ratios significantly ($p < 0.05$) below 1 after the application of DTT are indicated by asterisks (*) in Fig. 4. The double-mutants with $K_{D,ob}/K_{D,pre}$ ratios less than 0.37, which corresponds to stabilization energies above 1 kT, are labeled with triangles (△) (Ranganathan et al., 1996). Stabilization energies above 1 kT are deemed sufficient

TABLE II

Dissociation Constants (K_D) for Cd^{2+} Block of Double Mutants Observed before and after DTT Reduction (Means ± SEM)

	Y401C		W402C		E403C	
	Observed K_D (μM)		Observed K_D (μM)		Observed K_D (μM)	
	Nonreduced	Reduced	Nonreduced	Reduced	Nonreduced	Reduced
W756C	$1.2 \pm 0.1 \times 10$ (3)	$1.2 \pm 0.1 \times 10$ (3)	$1.4 \pm 0.1 \times 10^2$ (3)	$1.4 \pm 0.2 \times 10^2$ (2)	$2.4 \pm 0.3 \times 10^2$ (4)	$2.4 \pm 0.2 \times 10^2$ (2)
1757C	2.1 ± 0.4 (5)*	2.1 ± 0.5 (2)*	n.e.	n.e.	$1.4 \pm 0.2 \times 10^2$ (7)	$1.1 \pm 0.3 \times 10^2$ (2)
E758C	$1.2 \pm 0.1 \times 10^3$ (8)*	$9.3 \pm 1.8 \times 10^{-1}$ (5)*	$2.5 \pm 0.7 \times 10^{-1}$ (7)*	$2.5 \pm 1.0 \times 10^{-1}$ (3)*	$1.6 \pm 0.9 \times 10^2$ (5)	$1.9 \pm 0.2 \times 10$ (5)*
W1239C	$7.8 \pm 5.5 \times 10^{-1}$ (5)*	1.1 ± 0.3 (3)*	$1.2 \pm 0.1 \times 10$ (7)*	$1.3 \pm 0.1 \times 10$ (3)*	$3.7 \pm 0.2 \times 10$ (6)	$3.2 \pm 0.2 \times 10$ (3)
M1240C	6.0 ± 0.3 (7)*	6.1 ± 0.1 (2)*	2.3 ± 0.7 (7)*	3.0 ± 0.1 (3)*	$1.6 \pm 0.4 \times 10^2$ (8)	$1.6 \pm 0.3 \times 10^2$ (3)
D1241C	4.7 ± 0.7 (5)*	6.3 ± 0.6 (4)*	$5.2 \pm 0.6 \times 10$ (9)*	$2.8 \pm 0.3 \times 10$ (4)*	$1.3 \pm 0.1 \times 10^2$ (9)*	$1.2 \pm 0.2 \times 10^2$(3)*
A1529C	$2.1 \pm 0.5 \times 10^2$ (4)*	2.1 ± 0.1 (3)*	$1.1 \pm 0.5 \times 10$ (5)	$1.2 \pm 0.2 \times 10$ (3)	$1.5 \pm 0.3 \times 10^3$ (7)*	5.9 ± 1.8 (3)*
G1530C	1.8 ± 0.6 (7)*	1.4 ± 0.4 (2)*	$4.4 \pm 0.5 \times 10$ (7)	$4.8 \pm 0.8 \times 10$ (2)	$3.6 \pm 1.7 \times 10^3$ (6)*	8.3 ± 1.2 (5)*
W1531C	4.2 ± 1.0 (7)*	4.2 ± 0.8 (3)*	$1.9 \pm 0.3 \times 10$ (8)*	6.4 ± 0.9 (3)*	$9.7 \pm 5.0 \times 10$ (7)*	6.4 ± 1.0 (6)*
D1532C	4.2 ± 1.4 (7)*	2.4 ± 0.3 (4)*	$3.0 \pm 1.0 \times 10$ (6)*	7.9 ± 3.6 (4)*	$5.1 \pm 1.6 \times 10^2$ (5)	7.2 ± 2.6 (4)*

Mutants that are statistically different ($p < 0.05$) from the predicted values are indicated by asterisks. Numbers in parentheses represent the number of determinations. n.e., no expression.

in magnitude to clearly identify pairs of side-chains capable of "cross-talking" or interacting by coordinately binding Cd^{2+} and therefore having their sulphur atoms approach one another to within 3.5 Å (Torchinsky, 1981; Careaga and Falke, 1992; Balaji et al., 1989; Shaw et al., 1992). Inspection of Fig. 4 shows remarkable patterns for interacting pairs of residue side-chains, suggesting considerable pore flexibility. For example, E403C cross-talks with four adjacent consecutive P-loop residues in D-IV while Y401C talks with the same residues although the stabilization energy was slightly below 1 kT for the Y401C/W1531C mutant. On the other hand, E758C and D1532C can communicate with three consecutive residues in D-I. Both Y401C and W402C are rather promiscuous, cross-talking with residues in all three domains, often with multiple consecutive residues. Assuming no major disruption of the channel pore by double-cysteine replacement, these results are inconceivable for pore models assuming fixed alignments between P-loops regardless of the underlying secondary

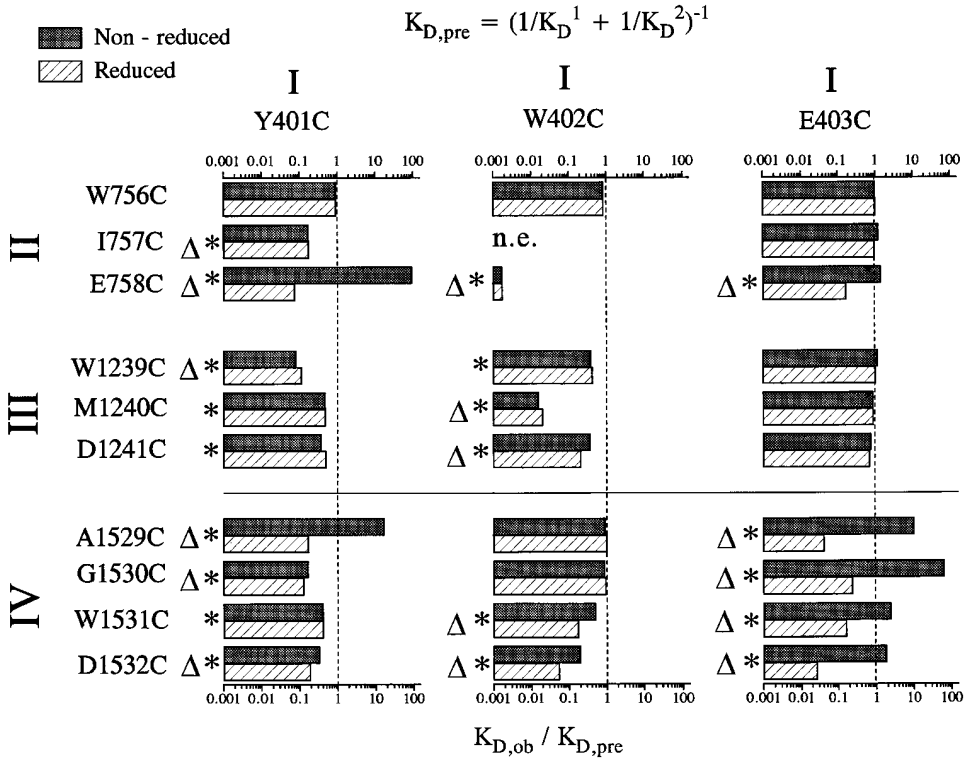

FIGURE 4. Ratios of the predicted dissociation constant, $K_{D,pre}$, to the experimentally observed dissociation constant, $K_{D,ob}$ for all the double mutants studied before (*filled bars*) and after (*open bars*) reduction by DTT. $K_{D,pre}$ is estimated from the dissociation constants recorded for the single-cysteine mutant channels assuming independent binding of Cd^{2+} to the inserted cysteines in double-cysteine mutants (see METHODS, Eq. 1). For the mutants with ratios of $K_{D,ob}/K_{D,pre}$ around 1, we assume that the two inserted cysteines are binding Cd^{2+} independently. Values of $K_{D,ob}/K_{D,pre}$ statistically different from 1 are identified by asterisks (*). The mutant channels with $K_{D,ob}/K_{D,pre}$ below 0.37 (i.e., with stabilization energies of 1 kT) are identified by open triangles.

structure and strongly suggest that P-loops in Na^+ channel pores are highly flexible.

Fig. 4 further shows that, in reduced channels, the $K_{D,ob}/K_{D,pre}$ ratio follows clear patterns which are well illustrated by double-mutants involving W402C and domain IV; $K_{D,ob}/K_{D,pre}$ is lowest for W402C/D1532C and progressively increases towards W402C/A1529C. This pattern suggests that Cd^{2+} coordination occurs most optimally for W402C interacting with D1532C and becomes increasingly more difficult for adjacent residues, probably due to the increased channel distortion required to trap the Cd^{2+} ion. Therefore, in spite of the large degree of P-loop flexibility in domain IV, W402 appears to interact preferentially with D1532, suggesting that W402 is physically closer to D1532 than to other D-IV residues. This preferential interaction pattern of a P-loop residue with specific residues in other domains is generally observed. Therefore, we can tentatively identify pairs of P-loop residues from distinct domains which are closely aligned. Generally, pairs of residues deemed as nearby neighbors are rarely at equivalent positions in the putative alignment sequence (Fig. 1). For example from the above arguments, W402 is judged to be most closely aligned with E758 in D-II, M1240 in D-III, and D1532 in D-IV, none of which are located at homologous locations in the alignment sequence shown in Fig. 1 *A*. This lack of correspondence between P-loop residues located at homologous locations in the different repeat domains of the Na^+ channel are consistent with previous single-channel results in single-cysteine mutant Na^+ channels (Chiamvimonvat et al., 1996).

Underlying Mechanism for the Enhanced Cd^{2+} Sensitivity in Double-mutant Channels

Single-channel recordings were used to establish the mechanism underlying the enhanced Cd^{2+} sensitivity of reduced Y401C/E758C mutants. Fig. 5 shows typical single-channel recordings at −80 mV for Y401C, E758C, and reduced Y401C/E758C channels recorded from inside-out cell attached patches in the absence (*A*) and presence (*B*) of Cd^{2+}. All recordings were made in the presence of 10 μM fenvalerate, which maintains Na^+ channels in the open state for tens to hundreds of milliseconds (Backx et al., 1992). For Y401C channels, Fig. 5 *B*

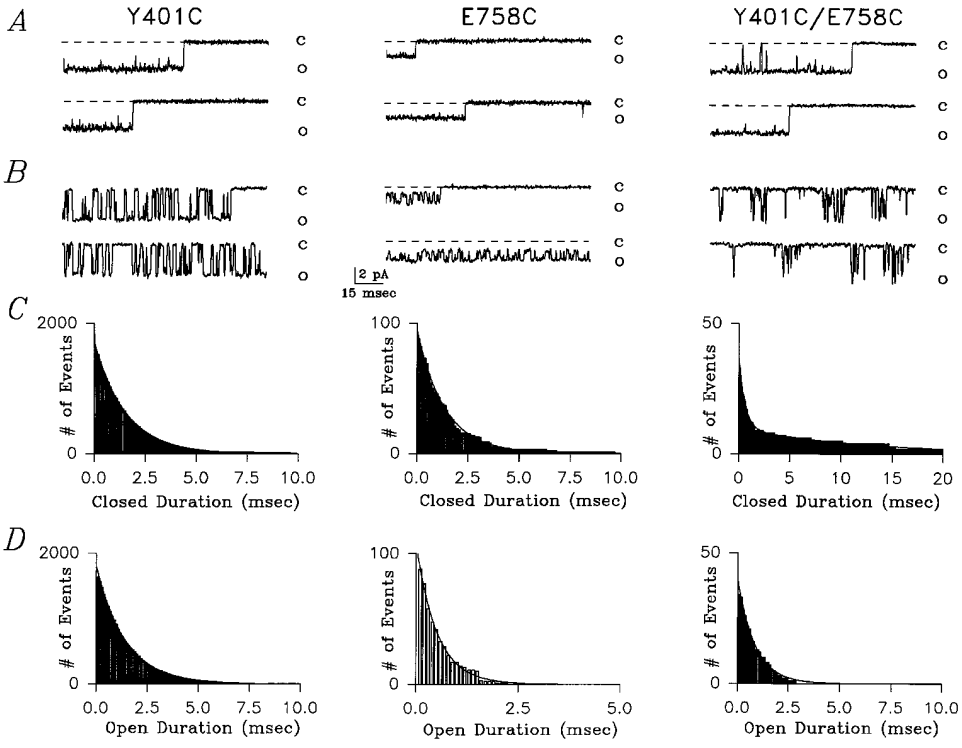

FIGURE 5. Single-channel recordings of Y401C, E758C, and reduced Y401C/E758C mutant channels following fenvalerate application at −80 mV. (*A*) Currents recorded in Y401C, E758C, and Y401C/E758C channels in the presence of 10 μM fenvalerate which is added to maintain the channels in the open state for tens to hundreds of milliseconds. (*B*) Currents recorded in Y401C and reduced Y401C/E758C mutants channels with 5 μM extracellular Cd^{2+} and in E758C channels with 400 μM Cd^{2+}. Cd^{2+} caused full closures of the Y401C and Y401C/E758C channels while blocking E758C channels to a sub-conductance level (closed level indicated by the *broken line*). In the presence of 5 μM Cd^{2+} the double-mutant channel Y401C/E758C displayed bursts of short-lived blocking events separated by long-lived blocking events not seen in either single-mutant. These long-lived blockages likely represent the "trapping" of the Cd^{2+} ion as a result of simultaneous interactions with the two free sulfhydryl groups. (*C*) The mean block-time histograms are shown for the channels illustrated in *A* for Y401C, E758C, and Y401C/E758C channels. The blocked-time histograms could be adequately fit using a mono-exponential equation for Y401C and E758C channels, while a bi-exponential function was required for Y401C/E758C channels. *Note:* the time axes are different in the different panels. See text for further details. (*D*) The mean unblocked-time (i.e., open-time) histogram is shown for the same channels illustrated in *B*. For Y401C, E758C, and Y401C/E758C channels the unblocked-time histogram could be adequately fit using a mono-exponential function.

shows representative single-channel sweeps measured in the presence of 5 μM Cd^{2+} in the pipette. Notice the discrete flicker blockade of the unitary current in Y401C channels (i.e., represented by *O*) often lasting several milliseconds which was not observed in the absence of Cd^{2+}. Cd^{2+} totally occludes the passage of Na^+ ions (i.e., represented by *C*) consistent with Cd^{2+} binding within the permeation pathway. The corresponding blocking-time histogram, illustrated in Fig. 5 *C*, could be adequately fit by a mono-exponential function, as expected if a single Cd^{2+} binding site exists within the pore. The estimated average block-time of Cd^{2+} ions within the pore (i.e., equal to the estimated time constant for the mono-exponential fit of the blocked-time histogram) was 1.43 ms for this Y401C (average 1.36 ± 0.12 ms, $n = 3$).

By contrast, E758C channels have a very different signature with respect to Cd^{2+} block. In the presence of 400 μM Cd^{2+}, E758C channels also show discreet reductions of unitary currents but these channels are blocked to a subconductance level establishing that Cd^{2+} binding to the channel does not fully prevent the passage of Na^+ ions (Fig. 5 *B*). The corresponding blocked-time histogram in Fig. 5 *C* was well fit with a mono-exponential function demonstrating that only a single Cd^{2+}-binding site exists within the pore of these channels. The average residence time estimated for the E758C patch shown in Fig. 5 *B* was 2.4 ms (average 2.21 ± 0.19 ms, $n = 3$).

By comparison with the corresponding single-cysteine mutant channels, reduced Y401C/E758C channels showed a very different blocking pattern. As depicted in Fig. 5 *B*, 5 μM Cd^{2+} caused complete interruptions of the unitary currents through reduced Y401C/E785C channels, like Y401C channels. However, simple inspection reveals that in these channels there are two distinct blocking times: repeated rapid closures are separated by very long-lived closures. As a result of these long closures, very little current passes through the channel in the presence of 5 μM Cd^{2+}, accounting for the very low dissociation constant measured for these channels following reduction (Fig. 3 *B*). The presence of two distinct blocking times is confirmed in Fig. 5 *C* which shows that adequate fitting to the blocked-time histogram required a bi-exponential function. The two estimated mean blocking times for this Y401C/E758C channel in the presence of 5 μM Cd^{2+} were 0.91 ms and 13.53 ms (average 1.10 ± 0.05 ms and 13.91 ± 0.09 ms, $n = 3$).

The presence of two distinct blocking times in reduced Y401C/E758C channels reveals the presence of two binding sites or two binding states of the channel. It is important to note that the smaller mean blocking time (i.e., 1.10 ms) in Y401C/E758C channels is similar to the mean blocking time Y401C channels (i.e., 1.32 ms) and that these short closures in Y401C/E758C channels fully occlude the unitary current as in Y401C channels. Therefore, it seems plausible that the rapid flicker blocking observed in the double-cysteine mutant channel are associated with Cd^{2+} binding to the inserted cysteine at position 401. This assertion is further bolstered by the absence of subconductance levels in the presence of Cd^{2+} and by the measured mean unblocked-time histograms (i.e., open-time histograms). Specifically, Fig. 5 *D* shows that in the presence of only 5 μM Cd^{2+} the mean unblocked-time for the Y401C and Y401C/E758C channels was 1.32 ms (average 1.22 ± 0.24 ms, $n = 3$) and 0.93 ms (average 1.05 ± 0.31 ms, $n = 3$), respectively, while in the presence of 400 μM Cd^{2+} the mean unblocked-time for E758C channels was 1.37 ms (average 1.21 ± 0.13 ms, $n = 3$). These mean unblocked-times yield estimates of the second-order rate constants for Cd^{2+} binding to the channels; for Y401C, E758C, and Y401C/E758C channels the second order rate constants for Cd^{2+} binding to the pore were 2.44×10^8 M^{-1} s^{-1}, 3.0×10^6 M^{-1} s^{-1}, and 2.1×10^8 M^{-1} s^{-1}, respectively. Thus it would appear that the rate of Cd^{2+} binding to the inserted cysteine at position 758 is too slow to contribute to the rapid blocking observed in Y401C/E758C channels exposed to 5 μM Cd^{2+}.

The very long average block-times (i.e., 13.91 ms) observed in Y401C/E758C channel are never observed in either of the corresponding single-cysteine mutants. Therefore, it seems likely that these events represent a novel binding state of the channel and probably represent coordinated trapping of the Cd^{2+} ion by simultaneous binding to C401 and C758 residues. Single-channel analysis on Y401C, E758C, and reduced Y401C/E758C channels reveals the probable kinetic events involved in simultaneous Cd^{2+} binding to the two pore cysteine side-chains: Cd^{2+} binds multiple times (i.e., average 3.4 times) to a single-cysteine residue (probably Y401C) for short durations followed occasionally by Cd^{2+} trapping as a result of simultaneous binding to C401 and C758 residues. Thus these observations provide direct information on the frequency of interaction of these two residues within the pore in the process of trapping a Cd^{2+} ion and demonstrate that models describing Cd^{2+} interactions with pairs of cysteine residues must consider both independent and simultaneous Cd^{2+} binding to the available sulfhydryls.

Relationship of P-loop Flexibility to Channel Function

While the data in Fig. 4 suggests P-loop flexibility, the functional importance of pore motion on channel behavior, as previously postulated (Läuger, 1987; Eisenman and Horn, 1983; Eisenman, 1984), remains speculative. The presence of cross-linkages for a number of

double-cysteine mutants provides a unique opportunity to further investigate the significance of pore motion. Indeed, we expect cross-linked channels to have reduced pore flexibility and motion compared to the same channels following reduction with DTT. As examples, Fig. 6, *A* and *C*, shows raw current traces following depolarization to −10 mV from a holding potential of −120 mV for E403C/D1532C and E403C/A1529C before (□, ○) and after (■, ●) disruption of the disulfide linkage with DTT. DTT application caused about a twofold and sixfold increase in peak current for E403C/D1532C and E403C/A1529C, respectively, indicating that these double-mutant channels are less capable of conducting current in the oxidized, cross-linked state versus the reduced state. The increase in whole-cell current following DTT exposure is not solely due to subtle changes in channel gating as illustrated in Fig. 6, *B* and *D*, which shows the current-voltage relationships for the corresponding mutants before (□, ○) and after (■, ●) the application of DTT. Not only is the peak of the current-voltage relationship significantly affected by DTT but the reversal potentials were also shifted: from 8 to 27 mV for E403C/D1532C and from 34 to 41 mV for E403C/A1529C after DTT application. Average shifts in reversal potential for 4 double-cysteine mutants and WT channels studied are summarized in Table III. Significant rightward shifts in reversal potential were observed in all cross-linked double-mutant channels, in which it was studied, following reduction with DTT. Furthermore, after reduction, the measured reversal potential closely matched the potential observed in the least selective of the corresponding single-cysteine mutants. Changes in selectivity following reduction could not be studied in cross-linked double-mutant channels involving cysteine replacements at position W1531 since W1531C channels are nonselective. Furthermore, 1.8-fold to 8-fold increases in whole-cell current were observed for cross-linked double-mutant channels (Fig. 4) following DTT exposure (data not shown) establishing that ionic conductance is strongly influenced by disulfide reduction. These results suggest that channel selectivity and permeation are impaired when channel motion is reduced by cross-linking. Alternatively, cross-linking of cysteine pairs could cause sufficient distortion of the P-loop structure to interfere with ion selectivity and permeation.

DISCUSSION

Many previous studies have assessed side-chain accessibility and local secondary structure of pore-forming regions in channels using cysteine-scanning mutagenesis by examining the pattern of accessibility of residues to reaction to sulfhydryl probes (Akabas et al., 1992; Gross

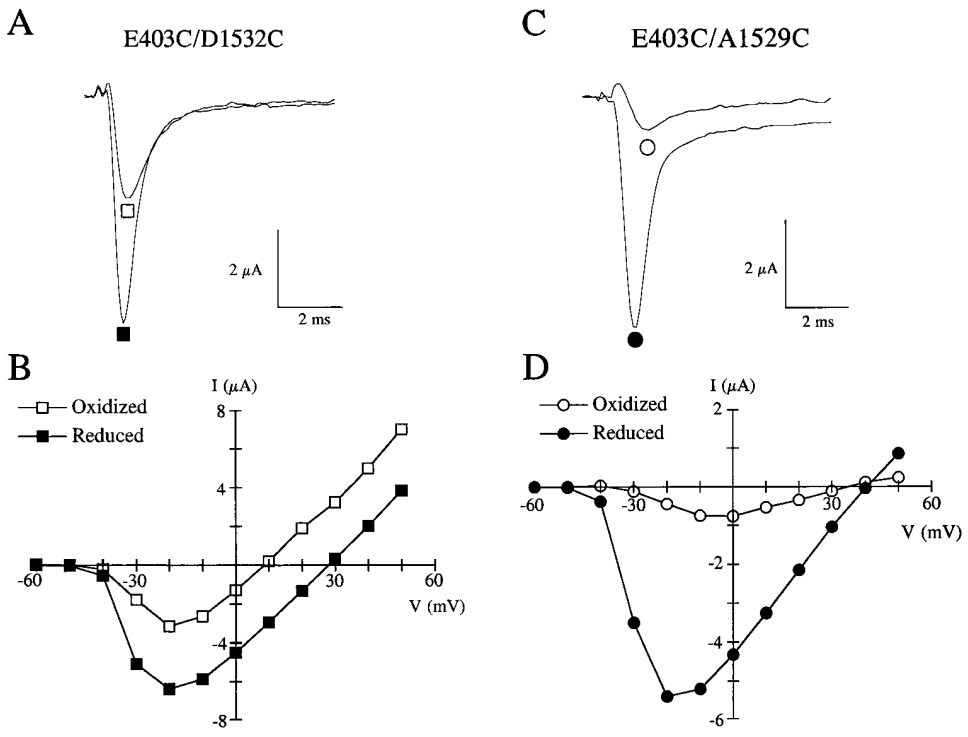

FIGURE 6. Effect of cross-linking on conductance and selectivity properties of double-cysteine mutants. (*A*) Raw current traces following depolarization to −10 mV from a holding potential of −120 mV for E403C/D1532C channels expressed in oocytes before (□) and after (■) reduction with DTT. Note the nearly twofold increase in current after reduction at this voltage. (*B*) The corresponding current-voltage relationships for E403C/D1532C. In this particular mutant, there is little change in the channel's conductance (161 μS before and 156 μS after DTT), estimated from the slope of the current-voltage curve at voltages above 0 mV, but the reversal potential is shifted by 19 mV to the right following reduction with DTT. (*C*) Raw traces for E403C/A1529C before (○) and after (●) the application of DTT. The current increased more than sixfold following reduction with DTT. (*D*) The current-voltage relationship for E403C/A1529C mutants shows a fivefold increase in slope at voltages above 0 mV (22 μS before and 97 μS after DTT), whereas the reversal potential is only slightly shifted rightward (7 mV) by reduction with DTT.

TABLE III

The Changes in the Reversal Potential before and after Treatment with 10 mM DTT in Cross-linked Double-cysteine Mutant Channels

Mutant	E_{rev} (−DTT)	E_{rev} (+DTT)	Observations
Wild-type	55.7 ± 3.6 mV	55.2 ± 2.9 mV	6
Y401C/E758C*	36.9 ± 7.5 mV	54.3 ± 8.5 mV	3
E403C/A1529C*	31.1 ± 4.9 mV	40.5 ± 4.2 mV	4
E403C/G1530C*	11.7 ± 6.7 mV	42.1 ± 7.4 mV	3
E403C/D1532C*	12.6 ± 6.1 mV	31.1 ± 6.6 mV	5

*Significantly different before and after DTT application ($p < 0.05$).

and MacKinnon, 1995; Kurz et al., 1995; Pascual et al., 1995; Perez-Garcia et al., 1996). In our experiments, all the single-cysteine mutant channels created, except W756C, (Fig. 1) showed enhanced sensitivity to block by extracellular application of Cd^{2+} when compared to wild-type channels. The enhancement of Cd^{2+} sensitivity in the single-cysteine mutants relative to WT channels ranged from no enhancement for W756C to a greater than 1,000-fold enhancement for Y401C channels. The basis for this variation in Cd^{2+} sensitivity between different single-cysteine mutant channels can be traced to differences in Cd^{2+} binding rates, unbinding rates or both. For example, Y401C is about 50-fold more sensitive to Cd^{2+} block than E758C, which results from a 100-fold faster Cd^{2+} binding rate (Fig. 5 *D*) and a 2-fold faster Cd^{2+} unbinding rate (Fig. 5 *C*) for Y401C compared to E758C channels. Alternatively, the difference in the Cd^{2+} binding affinity between Y401 and W402C can be traced primarily to a 40-fold increase in the Cd^{2+} unbinding rate from W402C channel compared to Y401C (Tomaselli et al., 1995). Generally, we found that both on- and off-rates for Cd^{2+} binding to the pore varied between different single-cysteine mutants as reported previously (Chiamvimonvat et al., 1996). The underlying molecular basis for these differences could relate to a number of factors such as variations in the dehydration/hydration rate, differences in the coordination of Cd^{2+} binding between mutants or varying degrees of exposure of the reactive sulfhydryls to the aqueous phase of the pore.

All single-cysteine mutant channels (except W756C) reacted with externally applied MTSEA which reduced, or eliminated, the enhanced Cd^{2+} sensitivity relative to WT channels. MTSEA application reduced the measured whole-cell current by varying amounts (i.e., 0.5-fold to 4-fold) in a time-dependent fashion for all the single-cysteine mutants except W756C. The rate of current reduction following MTSEA application varied between mutants, but the current invariably reached steady-state in less than 3 min. Thus all residues accessible to Cd^{2+} could be readily modified by MTSEA.

Our results confirm that multiple consecutive residues in the P-loops of all four domains have their side-chains exposed to the Na^+ channel pore (Chiamvimonvat, et al., 1996; Perez-Garcia et al., 1996). At first glance, these findings suggest that the secondary structure of these P-loops are not α-helices or β-strands as concluded by previous studies in Na^+ (Perez-Garcia et al., 1996) and K^+ channels (Gross and MacKinnon, 1995; Kurz et al., 1995; Pascual et al., 1995; Soman et al., 1995). However, conclusions based on cysteine-scanning studies have often implicitly assumed that the pore is a static structure which, as discussed below, is not the case for P-loops in Na^+ channels.

Identification of interacting pairs of inserted cysteines in distinct P-loops of the Na^+ channel pore revealed a pattern which cannot be explained by static pore structures. Regardless of the secondary structure of P-loops in Na^+ channel pores, geometric and stearic constraints prevent side-chains of three or four consecutive residues in a given P-loop from simultaneous coordinately binding Cd^{2+} with a single residue in another P-loop without backbone motion and flexibility (Creighton, 1993). The amount of movement required to account for our observations depends on the local secondary structure assumed but, for extended loop structures, requires residues to translate a minimum of 7 Å over-and-above that allowed by side chain motion. These estimates were obtained from simulations of random coils structures using the program Hyperchem™ (Hypercube Inc., Waterloo, Canada), where we examined the minimal distance which sulfur atoms on cysteine side-chains of four consecutive residues are required to translate in order to interact with a single point. Therefore, our double-cysteine substitution experiments in Na^+ channels establish that, on the time-scale of Cd^{2+} binding and coordination shown in Fig. 5 (i.e., several milliseconds), the P-loops are flexible structures, particularly for the P-loops in D-I and D-IV. As a result, cysteine-scanning mutagenesis experiments in Na^+ channels, using techniques involving irreversible modification of inserted cysteines (which occurs on a seconds to minutes time scale) and high affinity binding to inserted sulfhydryls by Cd^{2+} (which occurs on a time-scale of milliseconds), makes it difficult to make definitive conclusions regarding the secondary structure or membrane-sidedness of pore-forming domains. These limitations are expected to be particularly serious when using aqueous-soluble covalent modifiers of free sulfhydryls since these agents could irreversibly trap the channel in a subset of reactive conformational states available to the channel pore which might not reflect the average or important conformations available for normal channel function.

Another related limitation of our experimental approach using single- and double-cysteine replacements as a strategy for unraveling pore structure, imposed by the existence of P-loop flexibility, is the possible existence

of induced fits. For example, Cd^{2+} binding to single-cysteine mutant channels and coordinated Cd^{2+} binding within the pore of double-cysteine mutant channels is expected to energetically induce conformations which distort the normal molecular channel architecture of the pore required for normal ion permeation and selectivity. This distortion is anticipated, in spite of the similarity between the ionic size between Na^+ and Cd^{2+} ions, because the high binding affinity of Cd^{2+} for the inserted free sulfhydryls. Pore flexibility could also promote induced fitting of channel pores when tightly binding to toxins thereby complicating the interpretation of experiments designed to examine relationships between pore residues using interactions with high affinity toxins (Gross and MacKinnon, 1995; Hidalgo and MacKinnon, 1995; Naranjo and Miller, 1996; Ranganathan et al., 1996).

Following reduction of double-cysteine mutant channels with DTT, channel currents were invariably increased (Fig. 6). In principal, the rate of re-oxidation could be used as a measure of the proximity of the inserted cysteine pairs (Careaga and Falke, 1992; Benitah et al., 1996; Krovetz et al., 1997). However after DTT washout, currents did not decrease noticeably over periods lasting greater than 10 min in the presence of ND96 solutions for any of the double mutant channels. We attempted to apply Cu^+/phenanthroline to enhance oxidation rates of inserted sulfhydryl pairs, but the oocytes invariably developed a large nonspecific leak current. In addition, the Cd^{2+} dose-response curves, which routinely took greater than 20 min to record, could be adequately fit with a binding equation assuming a single binding site. Had partial re-oxidation taken place during the time-course of these experiments, the Cd^{2+} dose-response curves should show evidence for the existence of two types of binding sites, one for oxidized channels and one for reduced channels, which was not observed.

The mechanism of Cd^{2+} coordination as illustrated in Fig. 5 reveals that Cd^{2+} trapping by a pair of cysteines does not occur each time the Cd^{2+} ion enters the pore. In the case of the Y401C/E758C channel, it appears that Cd^{2+} binds in bursts followed by long-lived closure events. It seems probable that the bursts involve Cd^{2+} binding to single cysteines inserted in the pore while the long-lived blocking events reflect coordinated trapping of the Cd^{2+} ion by the two inserted cysteines. Therefore, the kinetic model which best explains coordinated Cd^{2+} binding in our double-cysteine experiments is:

$$\begin{array}{ccc} O_{401}{:}O_{758} + Cd^{2+} & \leftrightarrow & O_{401} - Cd{:}O_{758} \\ \updownarrow & & \updownarrow \\ O_{401}{:}O_{758} - Cd & \leftrightarrow & O_{401} - Cd - O_{758} \end{array}$$

where $O_{401}{:}O_{758}$ is the unblocked channel, $O_{401}-Cd{:}O_{758}$ is the channel with a Cd^{2+} bound to the Y401C position, etc. Our experimental results demonstrate that $O_{401}{:}O_{758}-Cd$ is rarely formed, as suggested by the absence of subconductance blocking events because the rate constant for Cd^{2+} binding to the E758C channels is about 100-fold slower than for Y401C channels. From these observations it is clear that Eq. 2, which is the correct dissociation constant for the formation of state $O_{401}-Cd-O_{758}$, does not correctly predict the experimentally observed dissociation constant for Cd^{2+} binding to the double-cysteine mutants as assayed by examining Cd^{2+} block of the whole-cell current.

The previous discussion highlights some practical experimental limitations which arise as a result of P-loop flexibility in Na^+ channels, but is flexibility important for Na^+ channel pore function (i.e., conductance and selectivity properties)? In other words, is flexibility observed in our double-cysteine experiments relevant on the time-scale of ions permeating the Na^+ channel? The active sites of many well-studied enzymes, including diffusion-limited enzymes, are comprised of intrinsically flexible random coils or loop structures (Branden and Tooze, 1991; Stone et al., 1992; Creighton, 1993; Wade et al., 1993; Arnold et al., 1994). Flexibility is essential for catalytic activity by influencing substrate binding, specificity, and sequestration (Welch et al., 1982; Branden and Tooze, 1991; Tanaka et al., 1992; Cottrell et al., 1995; Lan et al., 1995; Larson et al., 1995) as well as stabilization of intermediate transitional states (Fresht, 1985). By analogy the flexible P-loops in Na^+ channels might play similar roles. The possibility of pore flexibility is consistent with dynamic models of channel pores, used previously to describe gramicidin (Eisenman and Horn, 1983) and acetylcholine channels (Eisenman, 1984), wherein ion permeation requires motion of both channel pores and ions (Läuger, 1987). Dynamic behavior could also explain "multi-ion" behavior of Ca^{2+} channels (Läuger, 1987), which appear to have only a single cation binding-site (Ellinor et al., 1995). The potentially important role of flexibility in pore function is supported by a number of observations: (*a*) current decreased by as much as eightfold whereas selectivity for Na^+ versus K^+ was impaired in many cross-linked channels compared to reduced non–cross-linked channels (Table III), (*b*) mutations in domain IV, which appears to be the most flexible, changed selectivity properties more profoundly than other domains (Tsushima et al., 1997), and (*c*) inspection of the amino acid sequence of P-loops reveals that the P-loop in D-IV (i.e., GWDG) has a very high probability of forming a relatively flexible β-turn loop structure (Creighton, 1993).

From statistical thermodynamic theory, it is clear that the magnitude of structural fluctuations depends di-

rectly on the time-scale of the observations; the likelihood of observing energetically unfavorable, large structural fluctuations depends directly on the length of the observation period. Indeed, large amplitude excursions and long-ranged collective motions have been previously observed in ordered α-helical structures in proteins with known crystal structures (Careaga and Falke, 1992) using a similar double-cysteine strategy where rates of disulfide (i.e., seconds to minutes time-scale) were used as measures of motion and flexibility. Since Cd^{2+} binding in our experiments occurs on a time-scale which is three-orders of magnitude slower than ion permeation, relatively large fluctuations in energy, and thus structure, will be surveyed by our Cd^{2+} coordination studies. However, channel flexibility (and therefore frequency of side-chain interactions) is probably under-estimated in our experiments because disulfide formation and coordinated Cd^{2+} binding require very restricted geometries (Torchinsky, 1981; Balaji et al., 1989; Careaga and Falke, 1992) and require many molecular collisions for reactions to occur (Careaga and Falke, 1992). Nevertheless, the kinetics of cross-linking (Torchinsky, 1981; Careaga and Falke, 1992) and Cd^{2+} coordination are too slow in comparison to the permeation process (sub-microsecond time scale) (Hille, 1992) to allow direct conclusions regarding the role of channel flexibility in ion permeation and selectivity.

Finally, P-loop flexibility might reflect or be related to gating-dependent changes since channel gating usually occurs on a millisecond time-scale as does Cd^{2+} coordination. Indeed, movement in the pore of voltage-gated K^+ channels occurs during C-type inactivation (Yellen et al., 1994). More recently P-loop motion has been directly measured in voltage-gated K^+ (Liu et al., 1996) and cyclic nucleotide-gated channels (Sun et al., 1996) using sulfhydryl modification. However, in our studies, the gating properties of cross-linked double-mutant channels was not noticeably altered compared to reduced or SkM1 channels.

Conclusion

Our studies demonstrate that P-loops in Na^+ channels are flexible structures on the time-scale of Cd^{2+} coordination of double-cysteine mutant channels. Clearly, non-static behavior of Na^+ channel pores must be considered in evaluating structure-function studies using cysteine substitutions combined with sulfhydryl reactive probes. Further studies will be required to assess the contribution of pore flexibility to channel properties like ion permeation, selectivity, and channel gating.

We thank Dr. P. Pennefather and C. Bear for helpful comments on our studies.

This work was supported by the Medical Research Council of Canada and the Tiffin Trust Fund for equipment support. P.H. Backx is a Scholar with MRC of Canada. R. Tsushima was supported by a fellowship from the Department of Medicine, University of Toronto.

Original version received 23 January 1997 and accepted version received 2 May 1997.

REFERENCES

Akabas, M.H., D.A. Stauffer, M. Xu, and A. Karlin. 1992. Acetylcholine receptor channel structure probed in cysteine-substituted mutants. *Science (Wash. DC).* 258:307–310.

Arnold, G.E., J.I. Manchester, B.D. Townsend, and R.L. Ornstein. 1994. Investigation of domain motions in bacteriophage T4 lysozyme. *J. Biomol. Struct. Dyn.* 12:457–474.

Backx, P.H., D.T. Yue, J.H. Lawrence, E. Marban, and G.T. Tomaselli. 1992. Molecular localization of an ion-binding site within the pore of mammalian sodium channels. *Science (Wash. DC).* 257:248–251.

Balaji, V.N., A. Mobasser, and S.N. Rao. 1989. Modification of protein stability by introduction of disulfide bridges and prolines: geometric criteria for mutation sites. *Biochem. Biophys. Res. Commun.* 160:109–114.

Benitah, J.P., G.F. Tomaselli, and E. Marban. 1996. Adjacent pore-lining residues within sodium channels identified by paired cysteine replacements. *Proc. Natl. Acad. Sci. USA.* 93:7392–7396.

Bogartz, R.S. 1994. An Introduction to the Analysis of Variance. Praeger Publishers Inc., Westport, CT. 233–348.

Branden, C., and J. Tooze. 1991. Introduction to Protein Structure. Garland Publishing Inc., New York. 11–77.

Careaga, C.L., and J.J. Falke. 1992. Structure and dynamics of Escherichia coli chemosensory receptors. Engineered sulfhydryl studies. *Biophys. J.* 62:209–216.

Catterall, W.A. 1995. Structure and function of voltage-gated ion channels. *Annu. Rev. Biochem.* 64:493–531.

Chiamvimonvat, N., M.T. Perez-Garcia, R. Ranjan, E. Marban, and G.F. Tomaselli. 1996. Depth asymmetries of the pore-lining segments of the Na^+ channel pore revealed by cysteine mutagenesis. *Neuron.* 16:1037–1047.

Colquhoun, D., and F.J. Sigworth. 1983. Fitting and statistical analysis of single-channel records. *In* Single-Channel Recording. B. Sakmann and E. Neher, editors. Plenum Press, New York. 191–263.

Cotton, F.A., and G. Wilkinson. 1992. Advanced Inorganic Chemistry: A Comprehensive Text 3rd ed. Interscience Publishers, New York. 503–527.

Cottrell, T.J., L.J. Harris, T. Tanaka, and R.Y. Yada. 1995. The sole lysine residue in porcine pepsin works as a key residue for catalysis and conformational flexibility. *J. Biol. Chem.* 34:19974–19978.

Creighton, T.E. 1993. Proteins: Structure and Molecular Properties. W.H. Freeman and Co. New York. 201–269.

Eisenberg, R. 1990. Channels as enzymes. *J. Membr. Biol.* 115:1–12.

Eisenman, G. 1984. Ion Transport Through Membranes. B. Pullman and K. Yagi, editors. Academic Press, New York. 101–129.

Eisenman, G., and R. Horn. 1983. Ionic selectivity revisited: the

role of kinetic and equilibrium processes in ion permeation through channels. *J. Membr. Biol.* 11:197–225.

Ellinor, P.J., J. Yang, W.A. Sather, T.F. Zhang, and R.W. Tsien. 1995. Ca^{2+} channel selectivity at a single locus for high affinity Ca^{2+} interactions. *Neuron.* 15:1121–1132.

Fersht, A. 1985. Enzyme Structure and Mechanism, 2nd ed. W.H. Freeman and Company, New York. 311–344.

Gross, A., and R. MacKinnon. 1995. Agitoxin footprinting the *Shaker* potassium channel pore. *Neuron.* 16:399–401.

Guy, H.R., and S.R. Durell. 1995. Structural models of Na^+, Ca^{2+} and K^+ channels. *In* Ion Channels and Genetic Diseases. D.C. Dawson and R.A. Frizzell, editors. Rockefeller University Press, New York. 1–16.

Heginbotham, L., T. Abramson, and R. MacKinnon. 1992. A functional connection between the pores of distinctly related ion channels as revealed by mutant K^+ channels. *Science (Wash. DC).* 258:1152–1155.

Heinemann, S.H., H. Terlau, W. Stühmer, K. Imoto, and S. Numa. 1992. Calcium channel characteristics conferred on the sodium channel by single mutations. *Nature (Lond.).* 356:441–444.

Hidalgo, P., and R. Mackinnon. 1995. Revealing the architecture of a K^+ channel pore through mutant cycles with a peptide inhibitor. *Science (Wash. DC).* 268:307–310.

Hille, B. 1992. Ionic Channels in Excitable Membranes, 2nd ed. Sinauer Associates, Sunderland, MA. 261–389.

Isacoff, E.Y., Y.N. Jan, and L.Y. Jan. 1991. Putative receptor for the cytoplasmic inactivation gate in the Shaker K^+ channel. *Nature (Lond.).* 353:86–90.

Krovetz, H.S., H.M.A. Vandongen, and A.M.J. Vandongen. 1997. Atomic distance estimates from disulfides and high affinity metal-binding sites in a K^+ channel pore. *Biophys. J.* 72:117–126.

Kunkel, T.A. 1985. Rapid and efficient site-specific mutagenesis without phenotypic selection. *Proc. Natl. Acad. Sci. USA.* 82:488–492.

Kurz, L.L, R.D. Zuhlke, H.J. Zhang, and R.H. Joho. 1995. Side-chain accessibilities in the pore of a K^+ channel probed by sulfhydryl-specific reagents after cysteine-scanning mutagenesis. *Biophys. J.* 68:900–905.

Lan, Y., T. Lu, P.S. Lovett, and D.J. Creighton. 1995. Evidence for a (triosephosphate-like) "catalytic loop" near the active site of glyoxalase I. *J. Biol. Chem.* 270:12957–12960.

Larson, E.M., F.W. Larimer, and F.C. Hartman. 1995. Mechanistic insights provided by deletion of a flexible loop at the active site of ribulose-1,5-biphosphate carboxylase/oxygenase. *Biochemistry.* 34:4531–4537.

Läuger, P. 1987. Dynamics of ion transport systems in membranes. *Physiol. Rev.* 67:1296–1331.

Lipkind, G.M., and H.A. Fozzard. 1994. A structural model of the tetrodotoxin and saxitoxin binding site of the Na^+ channel. *Biophys. J.* 66:1–13.

Liu, Y., M.E. Jurman, and G. Yellen. 1996. Dynamic rearrangement of the outer mouth of a K^+ channel during gating. *Neuron.* 16: 859–867.

Lopez, G.A., Y.N. Jan, and L.Y. Jan. 1994. Evidence that the S6 segment of the voltage-gated K^+ channel comprises part of the pore. *Science (Wash. DC).* 367:179–182.

MacKinnon, R. 1991. Determination of the subunit stoichiometry of a voltage-activated potassium channel. *Nature (Lond.).* 350:232–235.

MacKinnon, R., and C. Miller. 1989. Mutant potassium channels with altered binding of charybdotoxin, a pore-blocking peptide inhibitor. *Science (Wash. DC).* 245:1382–1385.

Miller, C. 1992. Ion channel structure and function. *Science (Wash. DC).* 258:240–241.

Naranjo, D., and C. Miller. 1996. A strong interacting pair of residues on the contact surface of charybdotoxin and *Shaker* K^+ channels. *Neuron.* 16:123–130.

Nicholson, L.K., T. Yamazaki, D.A. Torchia, S. Grzesiek, A. Bax, S.J. Stahl, J.D. Kaufman, P.T. Wingfield, P.Y.S. Lam, P.K. Jadhav, et al. 1995. Flexibility and function in HIV-1 protease. *Nature Structural Biology.* 2:274–280.

Noda, M., S. Shimizu, T. Tanabe, T. Takai, T. Kayano, T. Ikeda, H. Takahashi, H. Nakayama, Y. Kanaoka, N. Minamino, et al. 1984. Primary structure of Electrophorus electricus sodium channel from cDNA sequence. *Nature (Lond.).* 312:121–127.

Pascual, J.M., C.C. Shieh, G.E. Kirsch, and A.M. Brown. 1995. K^+ pore structure revealed by reporter cysteines at inner and outer surfaces. *Neuron.* 14:1055–1063.

Perez-Garcia, M.T., N. Chiamvimonvat, E. Marban, and G.F. Tomaselli. 1995. Structure of the sodium channel pore revealed by serial cysteine mutagenesis. *Proc. Natl. Acad. Sci. USA.* 93:300–304.

Pompliano, D.L., A. Peyman, and J.R. Knowles. 1990. Stabilization of a reaction intermediate as a catalytic device: definition of the functional role of the flexible loop in triosephosphate isomerase. *Biochemistry.* 29:3186–3194.

Ranganathan, R., J.H. Lewis, and R. MacKinnon. 1996. Spatial localization of the K^+ channel selectivity filter by mutant cycle-based structure analysis. *Neuron.* 16:131–139.

Satin, J., J.W. Kyle, M. Chen, P. Bell, L.L. Cribbs, H.A. Fozzard, and R.B. Rogart. 1992. A mutant of TTX-resistant cardiac sodium channels with TTX-sensitive properties. *Science (Wash. DC).* 256: 1202–1205.

Shaw, C.F., III, M.J. Stillman, and K.T. Suzuki. 1992. Metallothioneins: Synthesis, Structure and Properties of Metallothioneins, Phytochelations and Metal-Thiolate Complexes. VCH Publishers Inc., New York. 1–13.

Soman, K.V., J.A. McCammon, and A.M. Brown. 1995. Secondary structure prediction of the H5 pore of potassium channels. *Protein Eng.* 8:397–401.

Stone, M.J., W.J. Fairbrother, A.G. Palmer III, J. Reizer, M.H. Saier, Jr., and P.E. Wright. 1992. Backbone dynamics of the Bacillus substilis glucose permease IIA domain determined from 15N NMR relaxation measurements. *Biochemistry.* 31:4394–4406.

Sun, Z.-P., M.H. Akabas, E.H. Goulding, A. Karlin, and S.A. Siegelbaum. 1996. Exposure of residues in the cyclic nucleotide-gated channel pore: P-region structure and function. *Neuron.* 16:141–149.

Tanaka, T., H. Yamaguchi, H. Kato, T. Nishioka, Y. Katsube, and J. Oda. 1993. Flexibility impaired by mutations revealed the multifunctional roles of the loop in glutathione synthetase. *Biochemistry.* 32:12398–12404.

Terlau, H., S.H. Heinemann, W. Stuhmer, M. Pusch, F. Conti, K. Imoto, and S. Numa. 1991. Mapping the site of block by tetrodotoxin and saxitoxin of sodium channel II. *Nature (Lond.).* 356: 441–444.

Tomaselli, G.F., H.B. Nuss, J.R. Balser, M.T. Perez-Garcia, K. Kluge, D.W. Orias, P.H. Backx, and E. Marban. 1995. A mutation in the pore of the sodium channel alters gating. *Biophys. J.* 68:1814–1827.

Torchinsky, Y.M. 1981. Sulfur in Proteins. Pergamon Press, Oxford. 1–98.

Trimmer, J.S., S.S. Cooperman, S.A. Tomiko, J. Zhou, S.M. Crean, M.B. Boyle, R.G. Kallen, Z. Sheng, R.L. Barchi, F.J. Sigworth, R.H. Goodman, W.S. Agnew, and G. Mandel. 1989. Primary structure and functional expression of a mammalian skeletal muscle sodium channel. *Neuron.* 3:33–49.

Tsushima, R.G., R.A. Li, and P.H. Backx. 1997. Altered ionic selectivity of the sodium channel revealed by cysteine mutations within the pore. *J. Gen. Physiol.* 109:463–467.

Vallee, B.L., and K.H. Falchuk. 1993. The biochemical basis of zinc physiology. *Physiol. Rev.* 73:79–118.

Wade, R.C., M.E. Davis, B.A. Luty, J.D. Madura, and J.A. McCammon. 1993. Gating of the active site of triose phosphate isomerase: Brownian dynamics simulations of flexible peptide loops in the enzyme. *Biophys. J.* 64:9–15.

Welch, G.R, B. Somogyi, and S. Damjanovich. 1982. The role of protein fluctuations in enzyme action: a review. *Prog. Biophys. Mol. Biol.* 39:109–146.

Yellen, G., M.E. Jurman, T. Abramson, and R. MacKinnon. 1991. Mutations affecting internal TEA blockade identify the probable pore-forming region of the K^+ channel. *Science (Wash. DC).* 251: 939–942.

Yellen, G., D. Sodickson, T.Y. Chen, and M.E. Jurman. 1994. An engineered cysteine in the external mouth of a K^+ channel allows inactivation to be modulated by metal binding. *Biophys. J.* 66: 1068–1075.